SECOND EUROPEAN CONFERENCE ON EARTHQUAKE ENGINEERING
AND SEISMOLOGY, ISTANBUL AUG. 25-29, 2014

INFLUENCE OF VIBRO STONE COLUMNS ON GROUND RESPONSE

Laurentiu FLOROIU[1] and Helmut SCHWEIGER[2]

ABSTRACT

The paper presents the preliminary findings of a qualitative investigation on how soil improvement by vibro stone columns influences ground response during earthquake events. The focus is kept on how modifications to stiffness, damping ratio and unit weight of the soil column reflect on the amplification function. Findings include the possibility that in certain conditions, the seismic loading on the superstructures could be decreased due to changes of the natural ground conditions, through consistent modifications to the amplification ratios and eigenfrequencies of the soil column.

INTRODUCTION

Ground response analyses are carried out mainly to determine the influence that site specific soil conditions have on the amplification of seismic action from bedrock to ground surface level. They provide important information for optimum earthquake design of structures.

It is quite common that foundation soils are improved (by means of stone columns, piles, jet grouting columns etc.) to increase bearing capacity and/or reduce settlements. Extensive work has also been done for investigation of the influence that these improvement solutions have on liquefaction, and are now regarded as reliable solutions for dealing with this engineering problem. But besides creating shorter drainage paths, reducing stresses in the unimproved soils etc., these improvement techniques will also have an influence on the foundation soil, and consequently on the structure, during an earthquake. For example, stone columns are constructed from granular material with expected higher damping ratio and stiffness than the ones of the natural soil. The anticipated soil behavior of such improved sites would include reduced displacement amplitudes and increased accelerations at surface level (Kramer 1996). A recent study (Vrettos 2013) concludes that near-surface increased rigidity due to foundation loads would have little influence on the fundamental natural frequency of a 2D soil model, but a consistent reduction of the amplification factor at the natural frequency.

This paper investigates, by means of the FE method, the way vibro stone columns (VSC), executed with the dry bottom-feed method (CEN 2005, EN 14731:2005), alter seismic site response in green field conditions. For this purpose, analytical, 1D frequency and time-domain, 2D and 3D time-domain analyses are performed, all employing an equivalent linear visco-elastic soil model. The considered soil improvement is modelled in the same framework, by means of individual continuum elements.

[1] Ing. Dipl., Keller Geotehnica S.R.L., Bucharest, l.floroiu@kellergeotehnica.ro
[2] Prof., Graz University of Technology, Institute for Soil Mechanics and Foundation Engineering, Graz, helmut.schweiger@tugraz.at

DESCRIPTION OF THE NUMERICAL MODEL

The analyzed soil profile is composed of a top 30m cohesive layer underlaid by rigid bedrock (v_{s0} > 800m/s, shear wave velocity for shear strains less than or equal to 1E-5, i.e. small strains). The mechanical parameters of the cohesive layer, constant over depth, fit to soil class D (CEN 2004, EN 1998-1:2004): v_{s0} = 150m/s, N_{SPT} < 15blows/30cm, c_u < 70kPa.

The horizontal acceleration-time history (PEER 2011) recorded during the 1989 Loma Prieta U.S.A. earthquake (Gilroy array #1, 090 CDMG station 47379) was used as input signal at rigid bedrock level. The signal used herein is illustrated in Figure 1, has a total length of 40.00s with a recording time step of 0.02s.

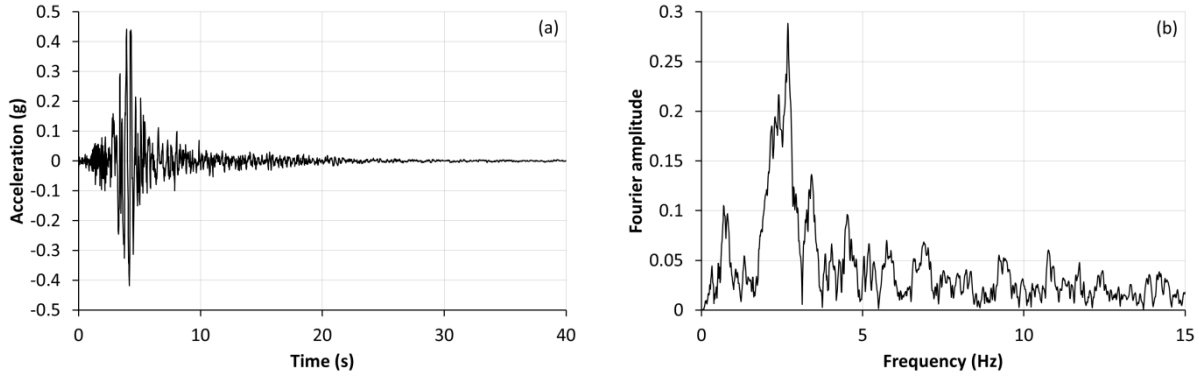

Figure 1. (a) Acceleration-time history and (b) Fourier amplitude of the seismic input

The results presented in this paper have been obtained with the aid of the finite element programs Plaxis 2D 2012 (Brinkgreve 2012) and Plaxis 3D 2013 (Brinkgreve 2013). The FE models are 720m wide and 30m deep, while the improved area is 150m wide and 15m deep, as shown in Figure 2. The soil improvement was modelled by means of individual continuum elements, with geometries shown in Table 1. The spacing and dimensions of the improvement elements were chosen so that the improved bodies, for the 2D and 3D models, have similar overall flexural rigidity (2D-1 and 3D-1, 2D-2 and 3D-2).

Table 1. Soil improvement scenarios

Soil improvement scenarios	**c/c** m	**w** m	**d** m	**Ar** m2	**t** m
2D-1	1.50	0.6	-	2.5	1.00
2D-2	3.00	0.6	-	5.0	1.00
3D-1	1.40	-	0.8	3.4	0.70
3D-2	2.34	-	0.8	10.9	1.17

, where c/c is center-to-center distance between improvement elements (rectangular grid), w is width of soil improvement element (2D, plane strain conditions), d is diameter of soil improvement element (3D), A_r is soil improvement replacement ratio (A_r=A/A_{SI}, where A is area of soil improvement cell and A_{SI} is area of soil improvement element) and t is model thickness.

The finite element meshes (Figure 3, Figure 4 and Figure 5) are composed of 6-noded triangular elements (2D) and 10-noded tetrahedral elements (3D). The average element size/length, l_e, is roughly 1.5m (2D) and 1.25m (3D) in the central 240m part of the model. The input accelerogram (Figure 1a) was applied with a constant amplitude throughout the model base, which was considered to be rigid bedrock level. Absorbent (viscous) boundaries (Lysmer 1969) were used on both sides of the model, which together with the relatively large model width aim to better replicate far-field conditions (bringing wave travelling direction closer to horizontal, in order to increase the efficiency of viscous boundaries). In this respect, both relaxation coefficients of the absorbent boundaries were considered equal to unity C_1=C_2=1 (Brinkgreve 2012). The implicit time integration scheme of Newmark was used with coefficients α=0.25 and β=0.5 as for the average acceleration method (Kontoe 2006, Brinkgreve 2012).

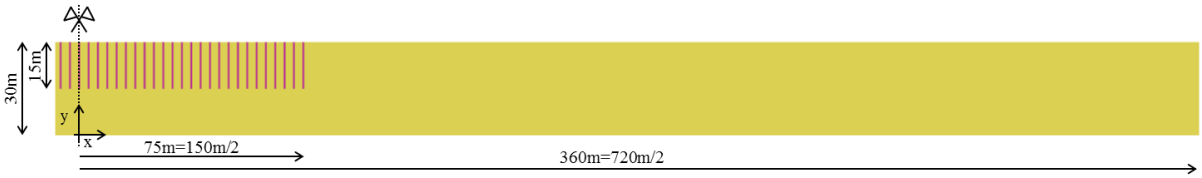

Figure 2. FE model geometry

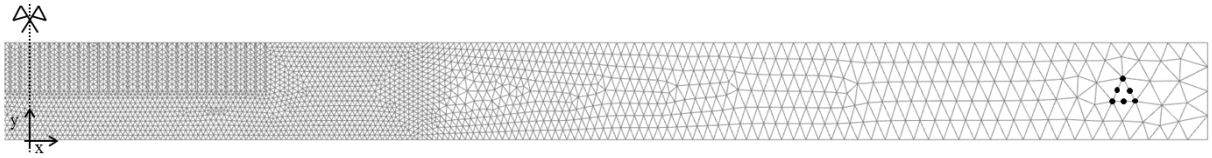

Figure 3. FE model mesh (2D)

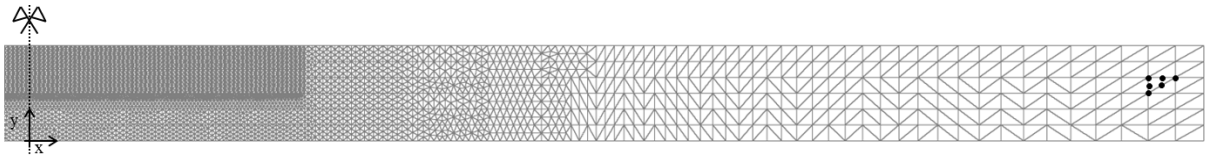

Figure 4. FE model mesh (3D)

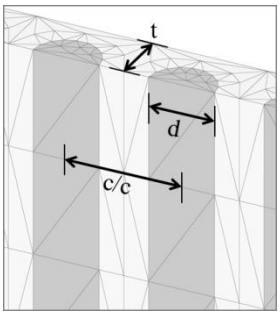

Figure 5. FE model mesh (3D). Detail

A linear visco-elastic model was used for all materials. In this framework, viscous damping is introduced by means of the frequency dependent Rayleigh formulation, which accounts for all types of material damping.

To determine stiffness and damping properties at seismic shear strain level (Table 2), the steps described below were applied:

- Evaluate stiffness parameters at small strains (G_0)
- Choose a representative shear strain level experienced during earthquake events (γ_{xy}=1E-3)
- Assess equivalent linear shear modulus and damping ratio (G, D) at seismic strain level (γ_{xy}), based on correlations of Seed and Indriss 1970, Vucetic and Dobry 1991, Darendeli 2001 and Zhang et al. 2005 (Figure 6 and Figure 7).

The average shear strain level considered as input for the previously described procedure (γ_{xy}=1E-3) is an estimation based on typical strain magnitudes recorded during earthquake events (Kramer 1996).

Table 2. Material properties

Material	**G_0** MPa	**ν** -	**γ** kN/m^3		**G/G_0** -	**G** MPa	**v_s** m/s	**E** MPa	**D** %
Unimproved soil, PI≤50% (soil class D, cohesive)	43.6	0.4	19		0.5	21.8	106	61	10
Granular material (VSC)	281.3	0.3	18		0.3	84.4	214	219	15

, where PI is plasticity index, G_0 is shear modulus at small strains, ν is Poisson's ratio, γ is unit weight, G is shear modulus at seismic strain level, v_s is shear wave velocity at seismic strain level, E is Young's modulus at seismic strain level and D is damping ratio at seismic strain level.

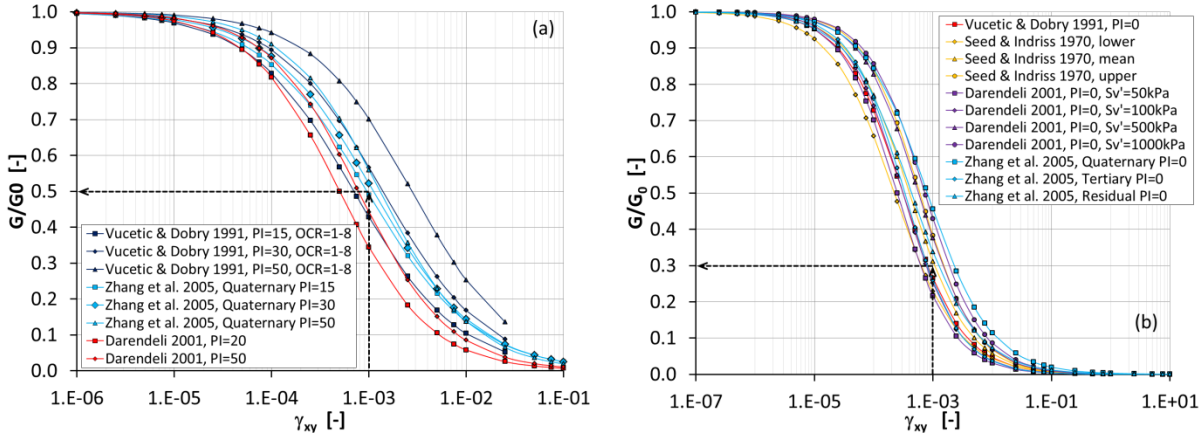

Figure 6. (a) Shear modulus variation with shear strain, for cohesive soils (PI≤50%), (b) Shear modulus variation with shear strain, for non-cohesive soils (Phillips 2009).

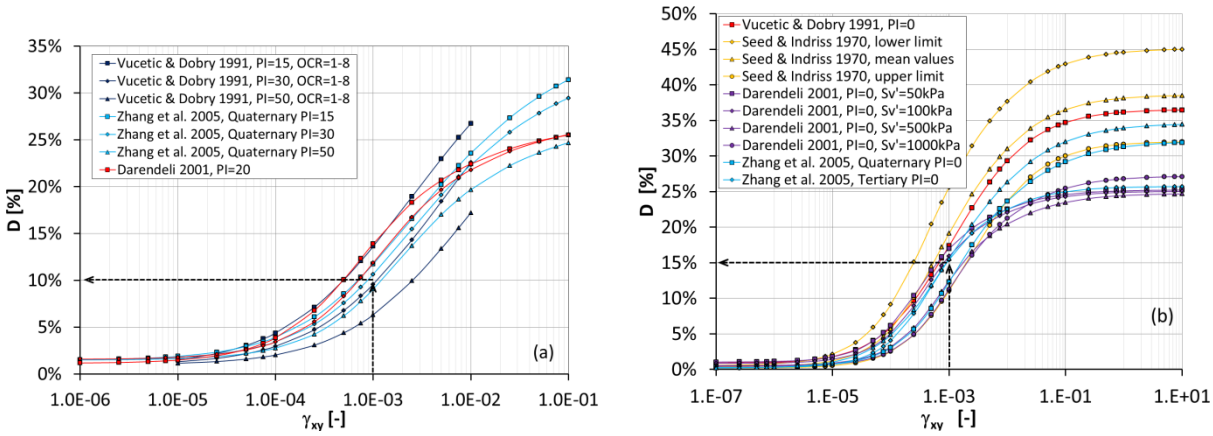

Figure 7. (a) Damping ratio variation with shear strain, for cohesive soils (PI≤50%), (b) Damping ratio variation with shear strain, for non-cohesive soils (Phillips 2009).

The first three eigenfrequencies of the unimproved soil model, based on the analytical solution (Roesset 1977), are f_1=0.88Hz, f_2=2.65Hz and f_3=4.42Hz. The amplification function was checked against the 1D frequency and time domain solutions (Hashash 2012), the 2D and 3D time domain FE solutions (Brinkgreve 2012), and the results (Figure 8) encouraged using the FE models for the next stage analyses.

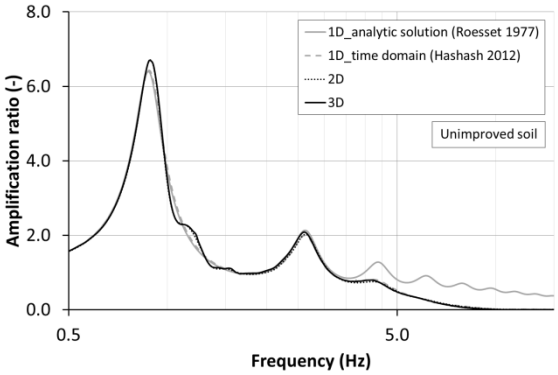

Figure 8. Amplification function for unimproved soil

Following the assessment of damping ratios at seismic strain level, the Rayleigh damping parameters (α_R and β_R) were calculated (Table 3 and Table 4) based on the first two eigenfrequencies (f_1 and f_2) of the improved soil, assessed at model's central position (Figure 11). Choosing to compute the Rayleigh damping from the first two eigenfrequencies of the model is related to both the frequency content of the seismic input signal and the area of interest of the ground response spectrum (Amorosi 2010). Therefore, it is expected that in this way, no significant variations of spectral accelerations will occur in the period interval 0.2s to 1.2s due to the frequency dependent Rayleigh damping.

Table 3. Material damping parameters for soil improvement scenarios 2D-1 and 3D-1

Material	**D** %		**f_1** Hz	**f_2** Hz	**α_R** -	**β_R** -
Unimproved soil	10		0.88	2.65	0.830	9.02E-3
Unimproved soil	10		0.88	2.93	0.850	8.36E-3
VSC	15				1.28	1.25E-2

Table 4. Material damping parameters for soil improvement scenarios 2D-2 and 3D-2

Material	**D** %		**f_1** Hz	**f_2** Hz	**α_R** -	**β_R** -
Unimproved soil	10		0.88	2.65	0.83	9.02E-3
Unimproved soil	10		0.88	2.68	0.833	8.94E-3
VSC	15				1.25	1.34E-2

The dynamic time step used in the implicit time integration scheme plays an important role for the reliability of the results. In order to avoid filtering of important seismic input, one must consider a small enough dynamic time step (δt), which in turn depends on (Brinkgreve 2012): the maximum frequency of interest (f_{max}), mesh coarseness (expressed as average element size/length, l_e) and stiffness of materials being travelled through by the seismic waves (expressed as compression and shear wave velocities, v_p and v_s). The FE programs' default values for the dynamic time step (i.e. number of sub steps, n) were used.

RESULTS AND DISCUSSIONS

The points of observation (element nodes) for the ground response analyses are shown in Figure 9, and their coordinates are as follows: x_A=0m, x_B=30m, x_C=60m, x_D=90m, x_E=120m, while y=30m for all. The points of observation which are positioned between the improvement elements, at level y=30m, show similar results to the ones positioned on top of the improvement elements, hence no differentiation is made between the two types of points.

Figure 9. Model observation points (2D & 3D models)

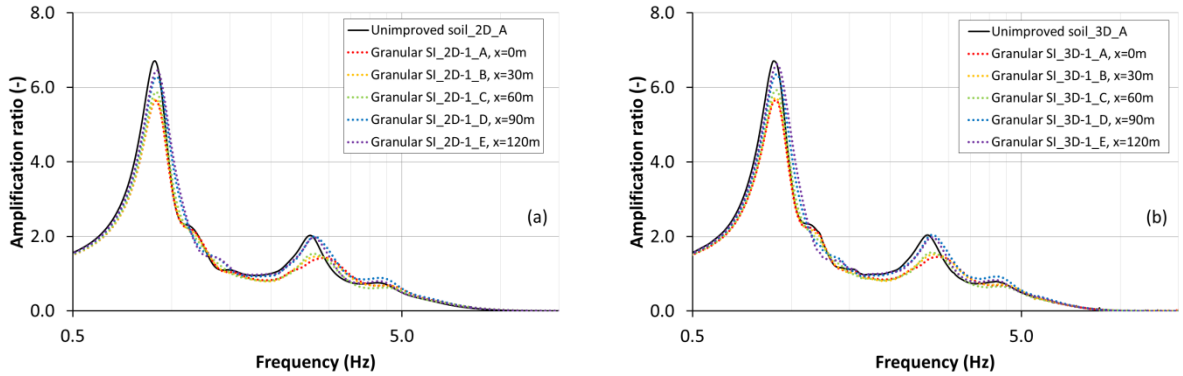

Figure 10. Amplification functions for unimproved soil and granular SI, at different observation points. (a) SI scenario 2D-1. (b) SI scenario 3D-1

The amplification functions for the granular soil improvement (SI) at each observation point, and for the unimproved soil, at the top central point of the models, are shown in Figure 10.

As it may be noticed in Figure 10, the effect of VSC consists in a decrease of amplification ratios, together with an increase of the second eigenfrequency (f_2) of the model. Also notable is the fact that soil improvement affects ground response rather uniformly throughout its width (observation points A, B, C) but also gradually extending beyond it (observation point D), up to a point where ground response becomes similar to the one of the unimproved soil (observation point E).

Figure 11 presents the results of all soil improvement scenarios, registered at top central position of the models (observation point A). In order to achieve similar analysis conditions for 2D and 3D models (2D-1 vs. 3D-1, 2D-2 vs. 3D-2), and consequently similar results, the improved zone (limited by x= -75…+75m and y=0…-15m) of the 3D models, compared to the 2D ones, was considered to have: a) similar flexural rigidity (already accounted for considered when setting up diameter and spacing of improvement elements) and b) similar damping ratio and unit weight, both averaged over improved volume. To achieve the later, the parameters of the unimproved soil between the improvement elements (within the improved zone) have been modified as show in Table 5.

Table 5. Modified parameters of unimproved soil between the improvement elements

Soil improvement scenarios		**γ** kN/m^3	**D** %
Granular SI	3D-1	18.7	11.0
	3D-2	18.9	10.6

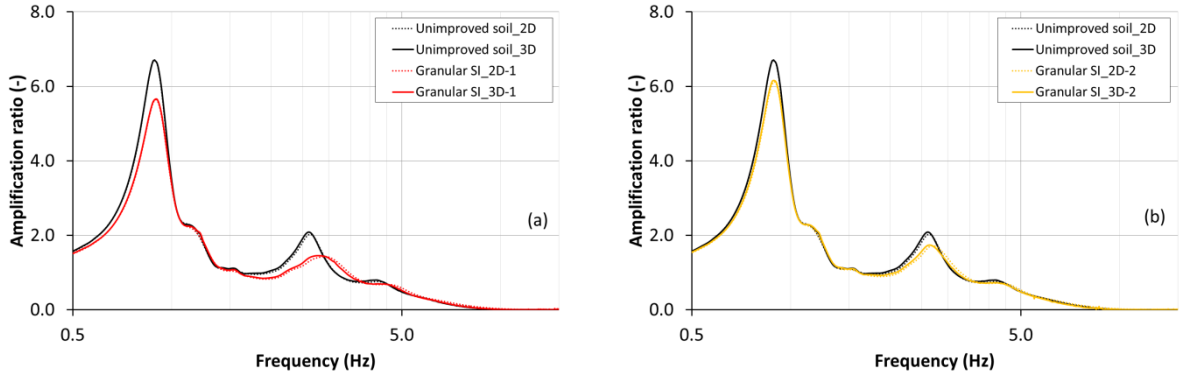

Figure 11. Amplification functions for unimproved soil and granular SI. (a) SI scenarios 2D-1 and 3D-1. (b) SI scenarios 2D-2 and 3D-2

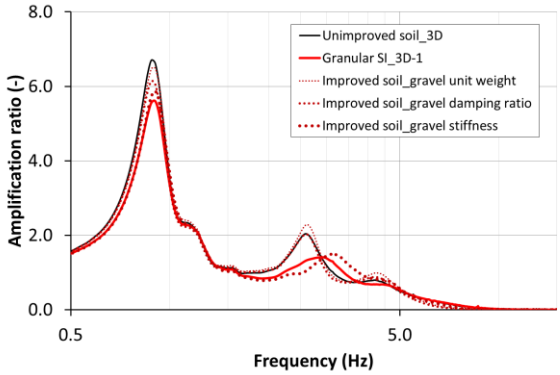

Figure 12. Influence of material parameters on amplification functions

One may observe the lower influence that soil improvement has on the amplification functions, as the soil improvement spacing decreases (2D-2, 3D-2 scenarios). Due to the reasonable agreement between results with 2D and 3D models (2D-1 vs. 3D-1, 2D-2 vs. 3D-2), from this point onward only results obtained with the 3D models are shown.

In order to investigate the reasons behind the modifications to amplification ratios and shift of models' higher order eigenfrequencies (f_2, f_3…), additional analyses were performed with the 3D-1 model (Figure 12). These analyses considered that the improvement elements have identical parameters to the unimproved soil, except one that is taken, analysis by analysis, from the parameter set of the granular material (unit weight, damping ratio and stiffness).

The investigation on the influence that individual material parameters have on amplification functions point to the following results:

a. the higher stiffness of the granular material, compared to the unimproved soil, generates a decrease of amplification ratio peaks and a shift of the higher order eigenfrequencies (f_2, f_3…);
b. the higher damping ratio of the granular material, compared to the unimproved soil, generates signal de-amplification without producing a shift of eigenfrequencies;
c. the marginally lower unit weight of the granular material, compared to the unimproved soil, has an insignificant effect on the amplification function;
d. the unimproved soil below the improved body dictates the model's first eigenfrequency (keeping it unchanged), independent of the soil improvement stiffness, damping ratio, unit weight and/or geometrical extent.

Figure 13 and Figure 14 show the spectral acceleration graphs resulted from the 3D models, registered at top central position (observation point A), together with the elastic response spectra (type 1) for soil classes C and D (CEN 2004, EN 1998-1:2004).

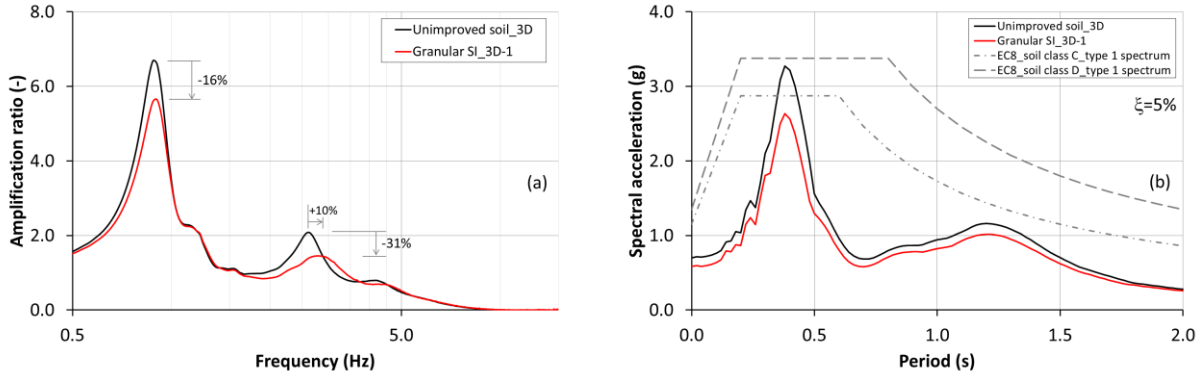

Figure 13. (a) Amplification functions and (b) spectral response, for unimproved soil and granular soil improvement (SI scenario 3D-1)

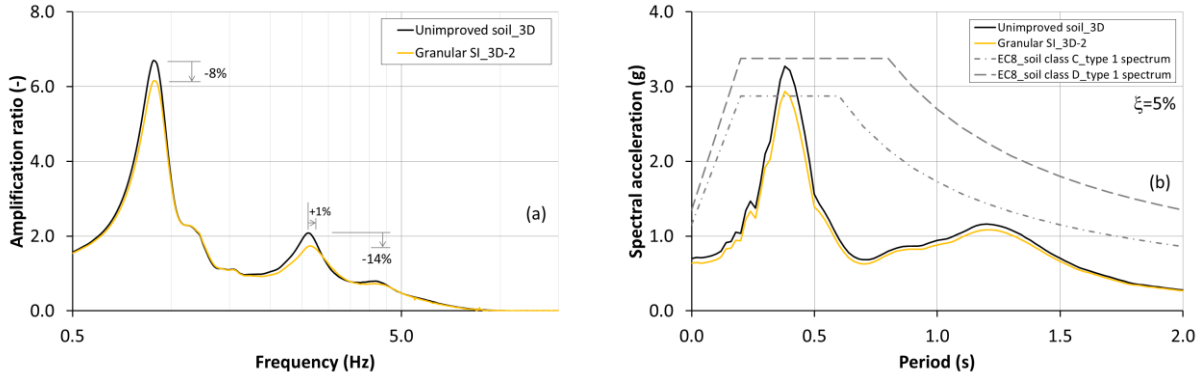

Figure 14. (a) Amplification functions and (b) spectral response, for unimproved soil and granular soil improvement (SI scenario 3D-2)

CONCLUSIONS

The paper presents the qualitative effects that soil improvement (vibro stone columns, executed with dry bottom-feed method), of specific geometric and material parameters, has on seismic ground response.

The main conclusions emerging from the obtained results are:

- increased stiffness of the improvement material is likely to decrease the amplification ratios around eigenfrequencies of the soil model, together with an increase of the higher order eigenfrequencies themselves (f_2, f_3 etc.);
- higher damping ratio of the granular material could decrease amplification ratios around the natural eigenfrequency of the soil model, without altering the eigenfrequencies;
- granular soil improvement seems to have the potential to reduce the seismic load on a building, when eigenfrequencies of soil model and structure have similar values;

Given the results presented herein it could be stated that the vibro stone columns have the potential, in certain conditions, to alter the local site effects. This could also be translated into a re-evaluation of site-specific soil classes, for structures that have their fundamental period in the vicinity of soil column's eigenperiods. The quantitative consequences of the current findings need to be investigated also with constitutive models that are able to account for irregular dynamic loading and with a consistent number of location-tailored seismic signals.

ACKNOWLEDGEMENTS

The authors acknowledge the support of Keller Grundbau GmbH Austria for the studies needed in preparation of this paper.

REFERENCES

Amorosi A, Boldini D, Gaetano E (2010) "Parametric study on seismic ground response by finite element modelling", *Computers and Geotechnics*, 37: 515-528

Antoniou S, Pihno R (2012) SeismoSignal 5.0, Seismosoft srl.

Brinkgreve RBJ, Engin E, Swolfs WM (2012) Plaxis 2D 2012, Plaxis bv.

Brinkgreve RBJ, Engin E, Swolfs WM (2013) Plaxis 3D 2013, Plaxis bv.

Bühler MM (2006) Experimental and Numerical Investigation of Soil-Foundation-Structure Interaction during Monotonic, Alternating and Dynamic Loading, PhD Thesis, Karlsruhe University, Karlsruhe, Germany

CEN, European Committee for Standardisation (2004), Eurocode 8: Design of structures for earthquake resistance – Part 1: General rules, seismic actions and rules for buildings, EN 1998-1:2004 E

CEN, European Committee for Standardisation (2005), Execution of special geotechnical works. Ground treatment by deep vibration, EN 14731:2005 E

Darendeli MB (2001) Development of a new family of normalized modulus reduction and material damping curves, PhD Thesis, University of Texas at Austin, U.S.A.

Hashash YMA, Groholski DR, Phillips CA, Park D and Musgrove M (2012) DEEPSOIL 5.1 User Manual and Tutorial, 107 pp

Kontoe S (2006) Development of time integration schemes and advanced boundary conditions for dynamic geotechnical analysis, PhD Thesis, Imperial College of Science, Technology and Medicine, London, U.K.

Kontoe S, Zdravkovic L, Potts DM, Menkiti CO and Lennon RF (2011) "Seismic response of complex soil-structure systems". *Proceedings of the 15th European Conference on Soil Mechanics and Geotechnical Engineering*, Athens, Greece, 12-15 September, 1491-1496

Kramer SL (1996) Geotechnical Earthquake Engineering, Prentice-Hall

Lysmer J and Kuhlemeyer RL (1969) "Finite dynamic model for infinite media", *Journal of Engineering and Mechanical Division ASCE*, 95 (EM4): 859–877

Pacific Earthquake Engineering Research Center – PEER (2011) Ground Motion Database – Beta Version, http://peer.berkeley.edu/products/strong_ground_motion_db.html

Phillips C and Hashas YMA (2009) "Damping formulation for nonlinear 1D site response analyses", *Soil Dynamics and Earthquake Engineering*, 29: 1143-1158.

Roesset JM (1977) "Soil amplification of earthquakes", Numerical Methods in Geotechnical Engineering, McGraw-Hill, New York, 639–682

Seed HB and Idriss IM (1970) Soil moduli and damping factors for dynamic response analyses, College of Engineering University of California Berkeley, U.S.A. 41pp.

Visone C, Bilotta E and de Magistris FS (2009) "One-Dimensional Ground Response as a Preliminary Tool For Dynamic Analyses in Geotechnical Earthquake Engineering" *Journal of Earthquake Engineering* 14: 131-162

Vrettos C (2013) "Dynamic response of sil deposits to vertical SH waves for different rigidity depth-gradients", *Soil Dynamics and Earthquake Engineering*, (47) 41-50

Vucetic M and Dobry R (1991) "Effect of soil plasticity on cyclic response", *Journal of Geotechnical Engineering* 117(1): 87-107

Zhang J, Andrus RD and Juang CH (2005) "Normalized shear modulus and material damping ratio relationships", *Journal of Geotechnical and Geoenvironmental Engineering* 131(4): 453-460